Effects of Stride Length and Running Mileage on a Probabilistic Stress Fracture Model

W. BRENT EDWARDS[1], DAVID TAYLOR[2], THOMAS J. RUDOLPHI[3], JASON C. GILLETTE[1], and TIMOTHY R. DERRICK[1]

[1]Department of Kinesiology, Iowa State University, Ames, IA; [2]Trinity Centre for Bioengineering, Department of Mechanical and Manufacturing Engineering, Trinity College Dublin, Dublin, IRELAND; and [3]Department of Aerospace Engineering, Iowa State University, Ames, IA

ABSTRACT

EDWARDS, W. B., D. TAYLOR, T. J. RUDOLPHI, J. C. GILLETTE, and T. R. DERRICK. Effects of Stride Length and Running Mileage on a Probabilistic Stress Fracture Model. *Med. Sci. Sports Exerc.*, Vol. 41, No. 12, pp. 2177–2184, 2009. The fatigue life of bone is inversely related to strain magnitude. Decreasing stride length is a potential mechanism of strain reduction during running. If stride length is decreased, the number of loading cycles will increase for a given mileage. It is unclear if increased loading cycles are detrimental to skeletal health despite reductions in strain. **Purpose**: To determine the effects of stride length and running mileage on the probability of tibial stress fracture. **Methods**: Ten male subjects ran overground at their preferred running velocity during two conditions: preferred stride length and 10% reduction in preferred stride length. Force platform and kinematic data were collected concurrently. A combination of experimental and musculoskeletal modeling techniques was used to determine joint contact forces acting on the distal tibia. Peak instantaneous joint contact forces served as inputs to a finite element model to estimate tibial strains during stance. Stress fracture probability for stride length conditions and three running mileages (3, 5, and 7 miles·d^{-1}) were determined using a probabilistic model of bone damage, repair, and adaptation. Differences in stress fracture probability were compared between conditions using a 2 × 3 repeated-measures ANOVA. **Results**: The main effects of stride length (P = 0.017) and running mileage (P = 0.001) were significant. Reducing stride length decreased the probability of stress fracture by 3% to 6%. Increasing running mileage increased the probability of stress fracture by 4% to 10%. **Conclusions**: Results suggest that strain magnitude plays a more important role in stress fracture development than the total number of loading cycles. Runners wishing to decrease their probability for tibial stress fracture may benefit from a 10% reduction in stride length. **Key Words:** BONE FATIGUE, OVERUSE INJURY, TIBIA, MUSCULOSKELETAL MODEL

Cyclical loads, such as those experienced by the skeletal system during running, have the potential to cause bone fatigue. Over time, material property degradation takes place (27,40) as microdamage manifests as small cracks in the bony matrix (6,31). With sufficient time for bone remodeling, this process may improve bone integrity through adaptation (4,9). However, if the accumulation of microdamage outweighs the rate of bone repair, microcracks may propagate into stress fractures (5,22).

Address for correspondence: William Brent Edwards, M.S., Department of Kinesiology, 283 Forker Building, Iowa State University, Ames, IA 50011-1160; E-mail: edwards9@iastate.edu.
Submitted for publication January 2009.
Accepted for publication April 2009.

0195-9131/09/4112-2177/0
MEDICINE & SCIENCE IN SPORTS & EXERCISE®

DOI: 10.1249/MSS.0b013e3181a984c4

The fatigue life of bone is inversely related to the applied mechanical load (7,8). When strain magnitudes are low, it is believed that microdamage accumulation will be limited and the tissue will have sufficient time to repair microcracks. Conversely, high strain magnitudes increase the rate of microdamage and, subsequently, overwhelm the repair process (15). Accordingly, identifying loading patterns that minimize strain magnitudes may aid in the prevention of stress fracture.

Decreasing stride length is a potential mechanism for bone strain reduction during running. Surrogate measures of bone strain, such as external ground reaction force and tibial shock, display positive relationships with stride length (12,23). The problem is that overuse injuries, such as stress fracture, are dependent on both loading magnitude and loading exposure. Because stride length reduction results in an increase in loading cycles for a given amount of mileage, it is unclear if such a kinematic adjustment would decrease the likelihood for stress fracture.

The purpose of this study was to determine the effects of stride length and running mileage on the probability of stress fracture at the tibia, a major site for stress fracture development (21,25). To this end, we investigated two stride lengths (preferred and −10% preferred) and three running regimens (3, 5, and 7 miles·d^{-1}; 4.83, 8.05, and 11.27 km·d^{-1}). We hypothesized that decreasing stride length by 10% would reduce the likelihood for stress fracture at each running mileage. We further hypothesized that increasing running mileage would increase the likelihood for stress fracture at each stride length.

METHODS

Stress Fracture Model

A probabilistic model of bone fatigue, repair, and adaptation was used to test our hypothesis. A step-by-step account of the equations and constants used within the model are introduced in the succeeding paragraphs. For a comprehensive review and theoretical development of the model, the reader is referred to Taylor (33), Taylor and Kuiper (35), and Taylor et al. (34).

Bone fatigue. The traditional means to describe the fatigue life of a material is with a stress–life plot or "*S–N* curve." A typical *S–N* curve can be expressed by the standard fatigue equation:

$$N_f = C\Delta\sigma^{-n} \quad [1]$$

where N_f is the number of cycles to failure, $\Delta\sigma$ is the stress range, n is the slope of the *S–N* curve, and C is a constant. Carter and Caler (7) observed a slope of $n = 6.6$ for fatigue damage of cortical bone at the large N_f values relevant to the present study.

Owing to inherent differences between experimental testing samples, considerable scatter in the number of cycles to failure at a given stress range can be obtained for similar specimens. Weibull (37) developed a statistical procedure to deal with the scatter associated with the fatigue of materials. Taylor's stress fracture model begins with a modified Weibull equation that accounts for stressed volume (33):

$$P_f = 1 - \exp\left[-\left(\frac{V_s}{V_{so}}\right)\left(\frac{\Delta\sigma}{\Delta\sigma^*}\right)^m\right] \quad [2]$$

where P_f is the cumulative probability that a volume of bone V_s will fail at stress ranging up to $\Delta\sigma$. The reference stress range $\Delta\sigma^*$ is a measure of the material strength defined as the stress range at which the probability for failure is 0.63 for a reference volume V_{so}. For a 96-mm^3 specimen of cortical bone from a relatively young (27 yr) individual, $\Delta\sigma^* = 86$ MPa for an endurance test of 100,000 cycles to failure (41). The Weibull modulus m expresses the degree of inherent scatter in the material's fatigue behavior. For human cortical bone, $m = 8$ (33).

Equation 2 refers to P_f at a particular $\Delta\sigma$ for a fixed number of loading cycles. For our purposes, it is more appropriate to obtain P_f for a given number of loading cycles at a fixed $\Delta\sigma$. Different $\Delta\sigma$ are related to N_f with equation 1. Dividing N_f by the number of loading cycles per day gives the time to failure t_f in days. Replacing $\Delta\sigma$ with t gives a Weibull equation of the form:

$$P_f = 1 - \exp\left[-\left(\frac{V_s}{V_{so}}\right)\left(\frac{t}{t_f}\right)^w\right] \quad [3]$$

where t_f is a function of both the material strength and applied stress range (34). In this equation, the Weibull modulus w is dependent on both the scatter in the data and the slope of the *S–N* curve ($w = m/n = 1.2$).

Like most materials, bone is subjected to loads that vary in amplitude. For example, bone stress during walking will be less than bone stress during running or jumping. To account for variable loading, Taylor and Kuiper (35) recommended using the concept of equivalent stress, in which a variable amplitude is transformed to an equivalent constant amplitude on the basis of a weighted average procedure:

$$\Delta\sigma_{eq} = \left(\frac{1}{N_T}\sum_{i=1}^{j}\left(N_i\ \Delta\sigma_i^n\right)\right)^{1/n} \quad [4]$$

where $\Delta\sigma_{eq}$ is the equivalent stress, N_i is the number of cycles at stress range $\Delta\sigma_i$, and N_T is the total number of cycles. This procedure assumes that the order in which the variable stress amplitudes are applied makes no difference on the fatigue life.

When dealing with whole bone, $\Delta\sigma$, and therefore P_f, is not constant throughout the entire bone. Using the finite element method, one can obtain a separate P_f for each element: call this P_i. If there are k elements, then P_f for the whole bone is the probability that any one element will fail, thus (35):

$$P_f = 1-(1-P_1)(1-P_2)(1-P_3)\cdots(1-P_k). \quad [5]$$

For convenience, elements experiencing similar stresses can be grouped together; Taylor and Kuiper (35) found that eight groups could be used without significant error. In practice, the researcher determines a $\Delta\sigma_{eq}$ and corresponding V_s for each of these eight groups before P_f calculation.

Bone repair. Bone repair is incorporated into the model with the use of a second Weibull equation:

$$P_r = 1 - \exp\left[-\left(\frac{t}{t_r}\right)^v\right] \quad [6]$$

where P_r is the probability of repair, the reference time for repair t_r is 26 d, and the Weibull modulus v is 2 (34). Written in terms of t, both P_f and P_r are the cumulative probabilities that failure or repair will occur from time 0 to t. To combine P_f and P_r, it is necessary to calculate the differential of P_f with respect to time or the "probability density function." The probability density function can be thought of as the probability that failure will take place within a unit period (e.g., 1 d). The bone will not fail if sufficient time has elapsed for repair to occur. Accordingly, the probability density function of failure with repair Q_{fr} is:

$$Q_{fr} = Q_f(1 - P_r) \quad [7]$$

where Q_f is the probability density function of failure. The cumulative probability of failure with repair P_{fr} is then:

$$P_{fr} = \int_0^t Q_{fr} dt \quad [8]$$

Bone adaptation. Deposition of new bone will occur on the periosteal surface in response to mechanical loading. In turn, the cross-sectional area and areal moment of inertia will increase such that the stresses experienced by the bone are reduced over time. To account for bone adaptation, the idea of $\Delta\sigma_{eq}$ is reintroduced. In the case of adaptation, $\Delta\sigma_{eq}$ can be calculated in integral form:

$$\Delta\sigma_{eq} = \left(\frac{1}{t_T}\int_0^{t_T} \Delta\sigma^n dt\right)^{1/n} \quad [9]$$

where t_T is the total time over which adaptation takes place (34). This is, in fact, the $\Delta\sigma_{eq}$ used within the model to determine the probability of failure with repair and adaptation P_{fra}.

Experimental Data Collection

Subjects. Ten experienced male runners were recruited for this study (age = 22.2 ± 3.2 yr, height = 1.8 ± 0.1 m, mass = 69.2 ± 6.5 kg), eight of which were former or current collegiate-level cross-country runners. All subjects were free from lower-extremity injury at the time of data collection. Before participation, subjects gave written informed consent and the study was approved by the institutional human subjects review board.

Data collection. Each subject was outfitted with a commercially available running shoe. A single researcher took anthropometric measurements and placed 13 retroreflective markers on anatomical landmarks of the subject's trunk and right lower extremity. Markers were adhered to the dorsi-foot, heel, medial and lateral malleolus, anterior calf, medial and lateral femoral epicondyle, anterior thigh, left and right greater trochanter, left and right anterior superior iliac spine, and the joint between the fifth lumbar and first sacrum (L5–S1). Preferred running speed and preferred stride length (PSL) were determined over a series of practice trials, during which the subjects ran along a 28.5-m runway. The subjects were asked to aim for a speed they would select for an 8- to 10-mile recovery run.

Subjects ran at their preferred running speed (4.4 ± 0.5 $m \cdot s^{-1}$) over a force platform (AMTI, Watertown, MA) during two conditions including PSL (3.1 ± 0.2 m) and 10% reduction in PSL (−10% PSL; 2.8 ± 0.2 m). Speed was monitored with motion capture using the horizontal component of the L5–S1 marker. Stride length manipulation was accomplished using tape adhered to the floor. Subjects were asked to land on the tape at a consistent location underneath their foot. Ten trials were performed at each condition, and trials were accepted if the speed was ±5% the preferred running speed and foot placement was visually reliable with tape location.

Motion capture data were collected with a Peak Motus 3D optical capture system (Vicon Peak, Centennial, CO) at a sampling frequency of 120 Hz. Force platform data were collected at a sampling frequency of 1200 Hz. The synchronized raw motion capture and force platform data were exported to MATLAB (The Mathworks, Natick, MA) for processing.

Musculoskeletal Modeling

Raw motion capture data were smoothed using a fourth-order zero-lag Butterworth filter with a low-pass cutoff frequency of 8 Hz. Ground reaction force data were smoothed in the same manner with a cutoff frequency of 50 Hz. A static trial was used to estimate joint center locations, and these were assumed to be stationary in the segmental coordinate systems. Three-dimensional Cardan segment and joint angles were calculated with a flexion/extension, abduction/adduction, internal/external rotation sequence. Joint moments and reaction forces were calculated using inverse dynamics and rigid body assumptions. The equations of Vaughan et al. (36) were used to obtain segment masses, center of mass locations, and moments of inertia.

The stance phase joint angles for each trial were interpolated to 1% increments and imported into a scaled SIMM 4.0 musculoskeletal model (MusculoGraphics, Inc., Santa Rosa, CA). For a detailed overview of the musculoskeletal modeling software, see Delp and Loan (11). The SIMM model was used to obtain maximal dynamic muscle forces, muscle moment arms, and muscle orientations for 43 lower-extremity muscles. The maximum dynamic muscle forces were adjusted for length and velocity. The information provided by SIMM was used to estimate individual muscle forces with a static optimization routine previously described by Edwards et al. (13).

Briefly, the static optimization routine used sequential quadratic programming. The cost function to be minimized was the sum of squared muscle stresses. Five joint moments determined from inverse dynamics were used to constrain the optimization. These included three orthogonal components of the resultant moment at the hip and one (flexion/extension) component at the knee and ankle. The lower bound and upper bound muscle forces were initially set to zero and the maximal dynamic muscle forces, respectively. The bounds were adjusted in subsequent frames to prevent nonphysiological changes in muscle force (29).

FEBio software (Musculoskeletal Research Laboratories, Salt Lake City, UT; http://mrl.sci.utah.edu/software.php?soft_id=7) was used to perform finite element analysis to calculate tibial strains. The tibia model consisted of 6340 nodes and 5391 hexahedral elements (VAKHUM data set; http://www.ulb.ac.be/project/vakhum/); the fibula was not considered. Material properties were assumed to be linearly elastic, with the cortical bone having an elastic modulus of 17 GPa, the trabecular bone having an elastic modulus of 1 GPa, and both materials having a Poisson's ratio of 0.3. A separate model was created for each subject, which was scaled to the individual's leg length. Each model was fully constrained at the tibial plateau, and a distributed joint contact force was applied to the distal tibia.

On the basis of previous research, Sasimontonkul et al. (30) concluded that approximately 10% of the ankle joint contact force is borne by the fibula. Therefore, the tibial contact force for running was calculated as follows:

$$\mathrm{Fc}_a = 0.09[\mathrm{RF}_a + \sum_{i=31}^{43} f_{ia}] \quad [10]$$

$$\mathrm{Fc}_s = 0.09[\mathrm{RF}_s + \sum_{i=31}^{43} f_{is}] \quad [11]$$

where Fc is the tibial contact force, RF is the ankle joint reaction force, and f_i is the ith predicted ankle joint muscle force (muscles i = 1–30 do not cross the ankle joint). Subscripts a and s denote axial and anterior–posterior (AP) shear components, respectively. Written in this form, RF and f_i are the forces in the leg coordinate system acting on the tibia. The medial–lateral (ML) shear component was not considered because subtalar moments were not used within the optimization routine. The mean peak instantaneous tibial contact forces for the 10 running trials were applied to the individual subject models.

Any cyclical loading, in addition to running, that takes place during daily activity will contribute to stress fracture development. To account for variable loading due to normal daily walking activity, tibial strains for normal and fast walking speeds were also determined. This has the effect of increasing the absolute accuracy in stress fracture prediction with the model. Walking tibial contact forces for fast walking speeds (0.9 × 4.6 body weight (BW)) were obtained from Glitsch and Baumann (16). The resulting strains were multiplied by a factor of 0.88 to obtain tibial strains for normal walking speeds, assuming a strain ratio equal to an external ground reaction force ratio between normal and fast walking speeds (38).

Applying the Stress Fracture Model

We assume that the bone is operating within its elastic range. Therefore, strain is proportional to stress and can be used in the stress fracture model equations provided constants such as C and $\Delta\sigma^*$ are converted.

The maximum absolute principal strains for walking and running were obtained for each element. Equation 4 was then used to obtain the element $\Delta\sigma_{eq}$. For each running condition, three mileages were investigated (3, 5, and 7 miles·d^{-1}). Running cycles per day were determined by dividing mileage by stride length. Walking cycles for normal (12,240 cycles per day) and fast (16,320 cycles per day) walking in athletic populations were obtained from Whalen et al. (38) and held constant across running conditions.

We found that we could accurately predict the ratio of compression to bending in our finite element model using beam theory. Assuming a maximum rate of lamellar bone deposition of 4 μm·d^{-1} (34), effectively changing the cross-sectional area and area moment of inertia, we determined an adaptation "strain ratio" for each day. The strain ratio was defined as the ratio of strain after bone deposition to strain with original bone geometry. This ratio was multiplied by the element strains to determine changes in tibial strain over time owing to bone adaptation. Equation 9 was then used to determine an equivalent strain for each element that accounted for adaptation.

All elements were separated into eight groups experiencing similar strain levels. The corresponding V_s for each group were obtained by summing individual element volumes within each group. Using the strain values from the midpoints of each group and the corresponding V_s (multiplied by 2 to account for both legs), equations 3 and 5 were

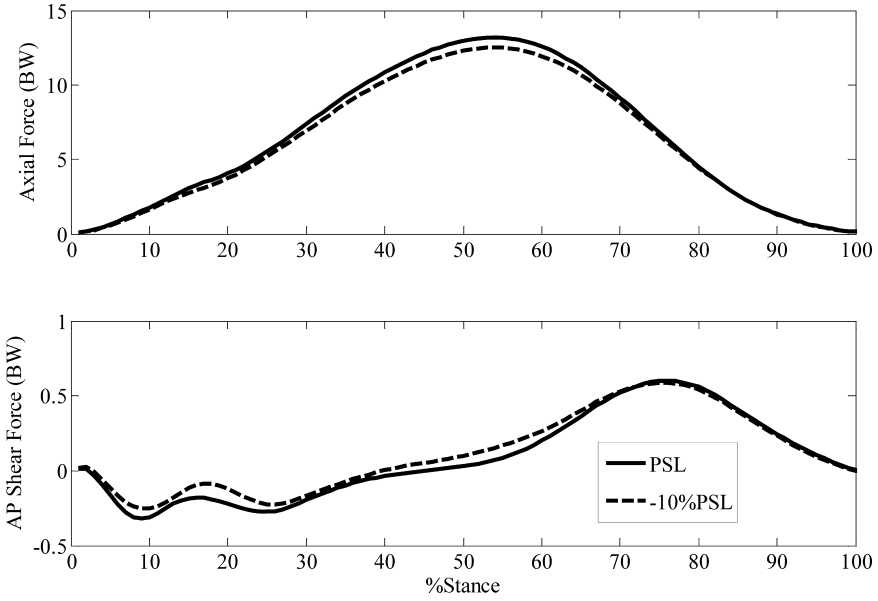

FIGURE 1—Ensemble average tibial contact forces for stride length conditions. Positive values represent axial compressive and anteriorly oriented shear force.

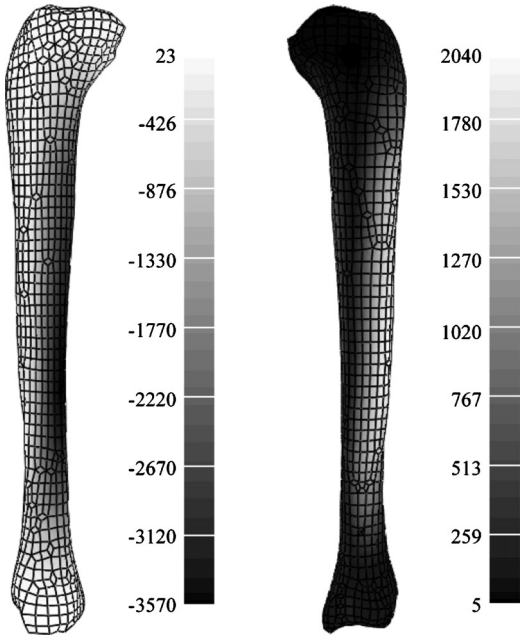

FIGURE 2—Sagittal views of a representative finite element model of the tibia displaying maximum principal strains (με) during running. The models were loaded in bending and axial compression with compression on the posterior surface (*left*) and tension on the anterior surface (*right*).

used to obtain P_f. Equations 6–8 were then implemented to obtain P_{fra}.

Statistics

Peak P_{fra} during the course of 100 d of training were determined for each running and mileage condition. Differences in P_{fra} were compared using a 2 × 3 repeated-measures ANOVA (2 stride lengths by 3 running mileages). Statistical analyses were performed in SPSS (SPSS, Inc., Chicago, Illinois) with the criterion α level set to 0.05. In the event of a significant main effect of running mileage, we used Bonferroni adjustments to assess pairwise comparisons of the estimated marginal means ($\alpha = 0.05/3 = 0.017$).

RESULTS

A 10% reduction in stride length resulted in a corresponding reduction in the peak resultant tibial contact force. For PSL, the peak Fc_a and Fc_s were 13.4 ± 1.2 BW and 0.1 ± 0.3 BW, respectively. Corresponding peak values for −10% PSL were 12.7 ± 1.0 BW and 0.1 ± 0.2 BW. Ensemble average tibial contact force profiles for both conditions are displayed in Figure 1.

For each subject, the finite element model was primarily loaded in bending with compressive strain on the posterior surface and tensile strains on the anterior surface (Fig. 2). Peak compressive principal strains ranged from 2800 to 4800 με during running conditions; peak compressive principal strains during walking were approximately 2.5 to 4.0 times lower.

The P_{fra} peaked and leveled off after approximately 40 d of running (Fig. 3). A significant interaction between stride length and running mileage was present ($P = 0.038$). Figure 4 shows that P_{fra} increased with running mileage at a faster rate during PSL. Because the resulting interaction was codirectional (i.e., the change in P_{fra} with increased mileage was in the same direction for both stride length conditions), interpretation of main effects is both appropriate and meaningful (19). For peak P_{fra}, the main effects of stride length ($P = 0.017$) and running mileage ($P = 0.001$) were significant. Bonferroni-adjusted pairwise comparisons of the estimated marginal means revealed significant differences between all mileages (mileages 3 to 5, $P = 0.008$;

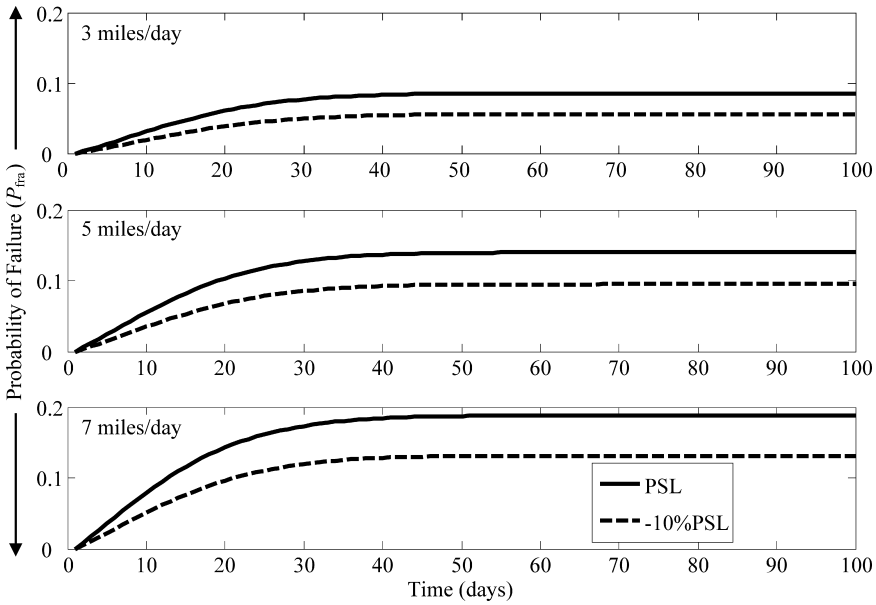

FIGURE 3—Ensemble average probabilities of failure (P_{fra}) across 100 d of training.

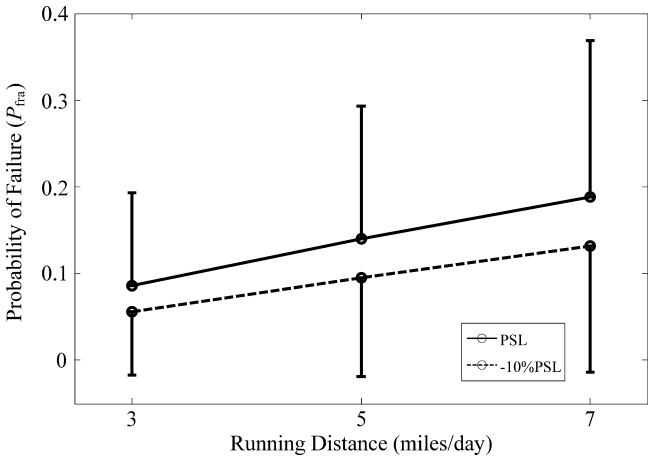

FIGURE 4—Mean peak probabilities of failure (P_{fra}). The likelihood for stress fracture increases with running distance at a faster rate during PSL.

mileages 3 to 7, $P = 0.004$; mileages 5 to 7, $P = 0.002$). A 10% reduction in PSL decreased the likelihood for stress fracture by 3% to 6% (Table 1). Increasing running mileage from 3 to 5 miles·d^{-1} resulted in an increase in stress fracture probability of 4% to 5%. Increasing running mileage from 3 to 7 miles·d^{-1} resulted in an increase in stress fracture probability of 7% to 10%.

DISCUSSION

The purpose of this study was to determine the effects of stride length and running mileage on the probability of stress fracture at the tibia. The results of this study suggest that a 10% reduction in PSL effectively reduces the likelihood for tibial stress fracture. This is true for weekly running mileages of 21, 35, and 49 miles·wk^{-1}. Not surprisingly, the probability for stress fracture increased with running mileage regardless of stride length condition. However, the rate at which P_{fra} increased with mileage was higher for PSL.

In general, stress fractures occur during the first 2 to 8 wk of a new training regimen (3). Annual incidence rates of stress fracture for male track and field athletes have been reported and range from approximately 10% to 20% (2,20). These studies found the tibia to be the most common site for stress fracture development. Our mean peak probability for tibial stress fracture across all conditions ranged from 6% to 20%, with P_{fra} peaking around day 40 (5.7 wk). Although this type of agreement between our modeling results and clinical findings is impressive, it would be unrealistic to try and predict actual stress fracture probability in individual runners with the current model. Table 1 illustrates the large between-subject variability found with this model; some explanations for this are presented in detail below. What is reliable with this type of modeling is the relative difference between conditions as indicated by the significant main effects of stride length and mileage.

The clinical implications for these results are clear. Those runners wanting to decrease their likelihood for stress fracture can do so by reducing their stride length by 10%. This reduction would also allow for runners to run an addition 2 miles·d^{-1} and maintain the same P_{fra}. The presence of the interaction further suggests that the benefits of reduced stride length are more pronounced at higher running mileages and this is most likely a direct effect of the nonlinear nature of the standard fatigue equation (equation 1). The difficulty for the clinician is in identifying those runners "at risk" for stress fracture that would benefit from a 10% stride length reduction. Presumably, these would be inexperienced runners beginning a weekly running routine or runners with a history of stress fracture. Poor physical fitness and low physical activity before physical training (32) and a previous history of stress fracture (24) are both associated with a higher risk of stress fracture development.

The metabolic cost of locomotion is optimized at preferred stride frequency and therefore PSL (17). If a 10% reduction in stride length were to increase the metabolic cost of running, it is likely that muscle fatigue would onset sooner in comparison to a PSL run. It has been argued that tensile muscle activity produces counteractive bending moments across long bones that help to lessen the peripheral stresses and strains. If the muscles fatigue, strains could potentially increase leading to a higher P_{fra}. Increased strains at the tibia after muscular fatigue have been empirically shown in both humans (26) and dogs (39). However, the work of Hamill et al. (17) showed that a 10% reduction in stride length does not significantly change oxygen consumption and HR from a PSL condition. We can thus conclude that the change in metabolic cost from a 10% reduction in stride length is negligible and that this type of kinematic adjustment would not accelerate the bone microdamage process through fatiguing muscles. However, if indeed strains were to increase during the run owing to muscular fatigue, the effects of running mileage within conditions would be exacerbated.

The basic motor pattern for locomotion is produced at the spinal level in mammals (28). Although these processes are somewhat "automatic" and subconscious, they can be overridden by higher-level brain activity for adaptive control. There is recent evidence to suggest that runners can improve faulty kinematics in as little as eight 10- to 30-min sessions of real-time visual feedback of kinematic data (10). These kinematic adjustments were maintained at a 1-month

TABLE 1. Mean (SD) peak probability of failure (P_{fra}).

Running Distance (miles·d^{-1})	PSL	−10% PSL
3	0.09 (0.11)	0.06 (0.07)
5	0.14 (0.15)	0.10 (0.11)
7	0.19 (0.18)	0.13 (0.15)

Main effects of stride length ($P = 0.017$) and running distance ($P = 0.001$) were significant. A significant interaction was also observed ($P = 0.038$).

follow-up free from visual feedback. We feel that a 10% reduction in PSL is a practical kinematic adjustment and one that could be successfully implemented using these types of gait retraining techniques.

There are several limitations that need to be borne in mind when interpreting the results of the current study. Of course, most of these limitations are minimized by the study's cross-over design (i.e., subjects serving as their own control). For example, we did not have subject-specific musculoskeletal model bone morphologies and material properties. Although the models were scaled to the subject's individual segment lengths, subtle differences in muscle orientations and moment arms could have lead to an overestimation or underestimation in individual muscle forces and, subsequently, tibial contact forces. Subject-specific material properties would have increased the accuracy in absolute stress fracture probability, and this may be one reason for the large running strains in certain subjects (i.e., 4800 με). *In vivo* research suggests that tibial strains rarely reach magnitudes higher than 2000 με at the anterior tibia; however, Ekenman et al. (14) observed tibial strains of 4200 με at the posterior tibia during forward jumping. Inclusion of individual muscle forces as boundary conditions within the finite element model could have also reduced our strains in specific areas of the tibia. Unfortunately, there is still much work to be done on the most appropriate way to load and constrain the tibia when using the finite element method.

The probabilistic stress fracture model is designed for runners beginning a running regimen. Because our subjects were mostly experienced level track and cross-country runners, it is likely that the microdamage repair process was already underway when they came in for laboratory testing. The same argument applies to the method we used to incorporate adaptation into the model. Future work could use more detailed modeling of bone adaptation, such as those proposed by Beaupre et al. (1) or Hazelwood and Castillo (18). Again, these limitations would not be expected to affect the relative differences between conditions and therefore influence the overall outcomes of the study. Although the study may have been improved by collecting walking data on our current subject pool, walking data were kept constant between running conditions, and a sensitivity analysis showed that manipulating the number of walking cycles per day had little effect on P_{fra}. Specifically, changing the time spent during normal and fast walking from 4 to 1 $h \cdot d^{-1}$ resulted in a percent change in stress fracture probability of less than 1%.

In conclusion, the results of our study suggest that a 10% reduction in PSL is an effective means to reduce the likelihood for stress fracture. Thus, it seems that the benefits of reducing strain with stride length manipulation outweigh the detriments of increased loading cycles associated with a given mileage. These benefits become more pronounced at higher running mileages. Our future work will focus on other practical kinematic alterations that may also reduce the probability for stress fracture.

Conflict of interest: The authors have no conflicts of interest.
No funding was provided for this research. The results of the present study do not constitute endorsement by ACSM.

REFERENCES

1. Beaupre GS, Orr TE, Carter DR. An approach for time-dependent bone modeling and remodeling-application: a preliminary remodeling simulation. *J Orthop Res*. 1990;8:662–70.
2. Bennell KL, Malcolm SA, Thomas SA, Wark JD, Brukner PD. The incidence and distribution of stress fractures in competitive track and field athletes. A twelve-month prospective study. *Am J Sports Med*. 1996;24:211–7.
3. Burr DB. Bone, exercise, and stress fractures. *Exerc Sport Sci Rev*. 1997;25:171–94.
4. Burr DB, Martin RB, Shaffler MB, Radin EL. Bone remodeling in response to *in vivo* fatigue microdamage. *J Biomech*. 1985; 18:189–200.
5. Burr DB, Milgrom C, Boyd RD, Higgins WL, Robin G, Radin EL. Experimental stress fracture of the tibia. *J Bone Joint Surg Br*. 1990;72-B:370–5.
6. Burr DB, Turner CH, Naick P, et al. Does microdamage accumulation affect the mechanical properties of bone? 1998;31:337–45.
7. Carter DR, Caler WE. A cumulative damage model for bone fracture. *J Orthop Res*. 1985;3:84–90.
8. Carter DR, Caler WE, Spengler DM, Frankel VH. Fatigue behavior of adult cortical bone: the influence of mean strain and strain range. *Acta Orthop Scand*. 1981;52:481–90.
9. Chamay A, Tschantz P. Mechanical influences in bone remodeling. Experimental research on Wolff's law. *J Biomech*. 1972; 5:173–80.
10. Crowell HP III, Davis IS. Reducing lower-extremity loads through gait retraining using real-time feedback methods. In: *Proceedings of the American Society of Biomechanics 30th Annual Meeting*. 2006 Sep: Blacksburg (VA). paper #318. Available from: http://www.asbweb.org/conferences/2006/pdfs/318.pdf.
11. Delp SL, Loan JP. A graphics-based software system to develop and analyze models of musculoskeletal structures. *Comput Biol Med*. 1995;25:21–34.
12. Derrick TR, Hamill J, Caldwell GE. Energy absorption of impacts during running at various stride lengths. *Med Sci Sports Exerc*. 1998;30(1):128–35.
13. Edwards WB, Gillette JC, Thomas JM, Derrick TR. Internal femoral forces and moments during running: implications for stress fracture development. *Clin Biomech (Bristol, Avon)*. 2008; 23:1269–78.
14. Ekenman I, Halvorsen K, Westblad P, Fellander-Tsai L, Rolf C. Local bone deformation at two predominant sites for stress fractures of the tibia: an *in vivo* study. *Foot Ankle Int*. 1998;19:479–84.
15. Frost HM. A brief review for orthopedic surgeons: fatigue damage (microdamage) in bone (its determinants and clinical implications). *J Orthop Sci*. 1998;3:272–81.
16. Glitsch U, Baumann W. The three-dimensional determination of internal loads in the lower extremity. *J Biomech*. 1997;30:1123–31.
17. Hamill J, Derrick TR, Holt KG. Shock attenuation and stride frequency during running. *Hum Mov Sci*. 1995;14:45–60.
18. Hazelwood SJ, Castillo AB. Simulated effects of marathon training on bone density, remodeling, and microdamage accumulation of the femur. *Int J Fatigue*. 2007;29:1057–64.
19. Hinkelmann K. *Evaluating and interpreting interactions* [Internet]. Blacksburg (VA):Virginia Polytechnic Institute and State University, Department of Statistics; 2004 [cited 2005 Jan 31]. Technical

Report No: 04-5. Available from: http://www.stat.org.vt.edu/dept/web-e/tech_reports/TechReport04-6.pdf.
20. Johnson AW, Weiss CB, Wheeler DL. Stress fractures of the femoral shaft in athletes-more common than expected: a new clinical test. *Am J Sports Med*. 1994;2:248–56.
21. Korpelainen R, Orava S, Karpakka J, Siira P, Hulkko A. Risk factors for recurrent stress fracture in athletes. *Am J Sports Med*. 2001;29:304–10.
22. Li G, Zhang S, Chen G, Chen H, Wang A. Radiographic and histological analyses of stress fracture in rabbit tibias. *Am J Sports Med*. 1985;13:285–94.
23. Mercer JA, Bezodis NE, Russell M, Purdy A, DeLion D. Kinetic consequences of constraining running behavior. *J Sports Sci & Med*. 2005;4:144–52.
24. Milgrom C, Giladi M, Chisin R, Dizian R. The long-term follow up of soldiers with stress fractures. *Am J Sports Med*. 1985; 13:398–400.
25. Milgrom C, Giladi M, Stein M, et al. Stress fractures in military recruits. *J Bone Joint Surg Br*. 1985;67-B:732–5.
26. Milgrom C, Radeva-Petrova DR, Finestone A, et al. The effect of muscle fatigue on *in vivo* tibial strains. *J Biomech*. 2007;40:845–50.
27. Pattin CA, Caler WE, Carter DR. Cyclic mechanical property degradation during fatigue loading of cortical bone. *J Biomech*. 1996;29:69–79.
28. Pearson K, Gordon J. Locomotion. In: Kandel ER, Schwartz JH, Jessell TM, editors. *Principles of Neural Science*. New York (NY): The McGraw-Hill Companies, Inc.; 2000. p. 737–55.
29. Pierrynowski MR, Morrison JB. A physiological model for the evaluation of muscle forces in human locomotion: theoretical aspects. *Math Biosci*. 1985;75:69–101.
30. Sasimontonkul S, Bay BK, Pavol MJ. Bone contact forces on the distal tibia during the stance phase of running. *J Biomech*. 2007; 40:3503–9.
31. Schaffler MB, Radin EL, Burr DB. Mechanical and morphological effects of strain rate on fatigue of compact bone. *Bone*. 1989; 10:207–14.
32. Shaffer RA, Brodine SK, Almeida SA, Williams KM, Ronaghy S. Use of simple measures of physical activity to predict stress fractures in young men undergoing a rigorous physical training program. *Am J Epidemiol*. 1999;149:236–42.
33. Taylor D. Fatigue of bone and bones: an analysis based on stressed volume. *J Orthop Res*. 1998;16:163–9.
34. Taylor D, Casolari E, Bignardi C. Predicting stress fractures using a probabilistic model of damage, repair and adaptation. *J Orthop Res*. 2004;22:487–94.
35. Taylor D, Kuiper JH. The prediction of stress fractures using a 'stressed volume' concept. *J Orthop Res*. 2001;19:919–26.
36. Vaughan CL, Davis BL, O'Connor JC. *Dynamics of Human Gait*. Champaign (IL): Human Kinetics; 1992. p. 84–5.
37. Weibull W. A statistical distribution function of wide applicability. *J Appl Mech*. 1951;18:293–7.
38. Whalen RT, Carter DR, Steele CR. Influence of physical activity on the regulation of bone density. *J Biomech*. 1988;21: 825–37.
39. Yoshikawa T, Mori S, Santiesteban AJ, et al. The effects of muscle fatigue on bone strain. *J Exp Biol*. 1994;188:217–33.
40. Zioupos P, Wang XT, Currey JD. Experimental and theoretical quantification of the development of damage in fatigue tests of bone and antler. *J Biomech*. 1996;29:989–1002.
41. Zioupos P, X TW, Currey JD. The accumulation of fatigue microdamage in human cortical bone of two different ages *in vitro*. *Clin Biomech (Bristol, Avon)*. 1996;11:365–75.